FULL PAPER

Studies on Chemical Modification of Porous Silicon-Based Graded-Index Optical Microcavities for Improved Stability Under Alkaline Conditions

T. Jalkanen, E. Mäkilä, Y.-I. Suzuki, T. Urata, K. Fukami, T. Sakka, J. Salonen, and Y. H. Ogata*

Preparation of graded-index optical microcavities based on porous silicon is demonstrated, and chemical modifications for obtaining improved stability under alkaline conditions are studied. Four surface modification methods for stabilizing the samples are examined, and the effects on the optical properties are verified. Two different thermal carbonization treatments resulting in hydrophilic and hydrophobic surfaces are employed. In addition, modification with undecylenic acid is performed on as-prepared and thermally hydrocarbonized porous silicon surfaces. Stability and sensing capabilities of the modified samples are examined by subjecting them to different concentrations of methylamine and trimethylamine vapors. Vapor induced changes in the reflectance spectra are used for evaluating sensitivity and stability. Sensitivity towards ethanol vapor is also measured in order to compare the sensitivity to a normal organic solvent. The results show that the two carbonization treatments and the undecylenic acid functionalization of the hydrocarbonized surface result in greatly improved stability. In contrast, derivatization of as-prepared porous silicon with undecylenic acid does not protect the surface sufficiently against oxidation under the highly basic conditions produced by the amine vapors. Surface chemistry is also shown to have a large effect on sensitivity towards the examined vapors. X-ray photoelectron spectroscopy was used to assess changes in elemental composition of sample surface. The results suggest that thermally promoted addition of undecylenic acid on hydrocarbonized porous silicon is an effective method for producing highly stable optical structures with a carboxyl group functionalization.

1. Introduction

Favorable optical properties, tunable surface chemistry, and large internal surface area of electrochemically prepared porous silicon (PSi) have led to the use of the material in chemical[1,2] and biochemical[3,4] optical sensing applications. Optical sensing is easily carried out by monitoring adsorption-induced changes in the reflectance spectrum of a PSi thin film or an interference reflector such as a Bragg reflector or a rugate filter.[5] In addition, PSi-based optical microcavities have also been employed in a variety of sensing applications.[6–8] PSi optical microcavities are usually prepared by fabricating a structure consisting of two Bragg reflectors and a spacer layer, which is located in the middle.[9–13] This defect inside the periodic structure acts as a resonant cavity which enables localization of the electromagnetic field.[14,15] Cavity-modes, which can be observed as narrow transmission lines inside the reflective stopband, are determined by the thickness of the layer. The conventional Fabry-Pérot filter structure requires careful control over thicknesses of individual layers on the Bragg reflectors and also over the thickness of the spacer layer, sandwiched between the reflectors. However, a graded-index approach could also be adopted, where rugate filters[16] would be used instead of Bragg reflectors. This approach is likely to be less sensitive to slight fluctuations in sample preparation conditions, as the main determining factor of a high quality resonant cavity is, in this case, the thickness of the cavity layer. The graded-index structure requires a gradually changing refractive index profile perpendicular to the sample surface, which is easily produced for PSi by using a programmable current source.[17,18] Graded-index microcavities have been modeled theoretically[16] and also demonstrated experimentally by glancing angle deposition of titanium dioxide.[19]

In long-term sensing applications the samples are required to exhibit sufficient stability. After the electrochemical anodization process the as-prepared PSi surface is covered with hydride species, which makes it susceptible to oxidation. This causes undesirable changes in many material properties of PSi.[20–23]

T. Jalkanen, E. Mäkilä, Prof. J. Salonen
Department of Physics and Astronomy
University of Turku
FI-20014 Turku, Finland
E-mail: jarno.salonen@utu.fi
T. Jalkanen, T. Urata, Prof. K. Fukami, Prof. T. Sakka, Prof. Y. H. Ogata
Institute of Advanced Energy
Kyoto University
Uji, Kyoto 611-0011, Japan
Dr. Y.-I. Suzuki
Central Research Laboratory
C. Uyemura & Co. Ltd., Hirakata, Osaka 573-0065, Japan
Prof. J. Salonen
Turku University Centre for Materials and Surfaces
University of Turku
FI-20014 Turku, Finland

DOI: 10.1002/adfm.201200386

In sensing applications this leads to gradual zero-point-drift of the sensor. Thermal oxidation is often used to passivate the PSi surface for chemical sensing applications, and it has been found as an effective stabilization method for optical vapor sensors.[24] However, due to solubility of silicon oxide under basic conditions[20], oxidation does not stabilize the structure for some biosensing applications. Alternative methods for increasing the stability of PSi surface have been obtained through the use of Si-C bonds.[21] Buriak et al. first demonstrated a Lewis acid mediated approach[25] to functionalizing the PSi surface, which was soon followed by a report on photopatterned hydrosilylation.[26] Both methods resulted in greatly increased stability of the PSi surface, even in boiling solutions of alkaline KOH. Soon after, a thermally promoted approach to hydrosilylation was proposed.[27–29] Boukherroub and co-workers also demonstrated derivatization of PSi with undecylenic acid, which enabled hydrophilic surfaces with greatly improved stability.[29] Later, treatment efficiency for functionalized PSi surfaces was further increased to approximately 80% by using so-called methyl capping, where residual Si-H surface species, which remained un-reacted during the initial treatment step due to steric hindrance, were replaced with methyl groups.[30]

Thermal carbonization (TC), which exploits small acetylene gas molecules, is an alternative approach for modifying the surface of PSi.[31–33] TC can be used to create either hydrophilic or hydrophobic PSi surfaces that display considerably improved stability. The resulting electrically conductive PSi surface has been utilized in developing electrical humidity sensors.[34–36] In addition, thermally carbonized PSi (TCPSi) electrical sensors have been found extremely sensitive to certain amine vapors.[37] TC treatment has also been proved effective in stabilizing PSi optical interference filters for sensing applications.[38,39] Recently, new approaches to surface functionalization that use the thermally hydrocarbonized[33] (THC) PSi have been demonstrated.[40,41] In these approaches, stability issues arising from incomplete surface coverage due to steric hindrance are circumvented by first stabilizing the PSi surface with the THC treatment. The Si-CH_x terminated surface can then be further functionalized by grafting molecules with functional moieties using, e.g., radical coupling of a dicarboxylic acid with a diperoxide initiator to obtain a partial carboxylic acid termination on the THCPSi surface[40] or by adopting the thermally promoted method in undecylenic acid[29,41] for the addition of acid termination. The -COOH -terminated THCPSi surface was demonstrated to be considerably more stable than an as-anodized PSi surface treated with thermal hydrosilylation of undecylenic acid.[40]

In this work, four chemical surface modifications for stabilizing PSi optical microcavities against alkaline environments are compared. TC- and THC-PSi optical microcavities are prepared and their stability and sensitivity towards methylamine (MA) and trimethylamine (TMA) vapors is evaluated. Also, thermally promoted addition of undecylenic acid (10-undecenoic acid) on PSi and THCPSi optical microcavity samples is performed, and sample stability and sensitivity towards amine vapors is examined. Ethanol (EtOH) vapor is used as a reference gas for comparing the sensitivities of the different chemically modified surfaces towards a common organic solvent. X-ray photoelectron spectroscopy (XPS) was used for evaluating surface composition and monitoring possible changes caused by the sensing experiments. The results demonstrate that surface chemistry has a clear effect on stability and sensitivity of the structures. Derivatization of THCPSi with undecylenic acid (UnTHC) was found to be a promising method for producing functionalized PSi surfaces with greatly improved stability and favorable optical properties.

2. Results

2.1. Effect of Surface Modifications on Microcavity Spectra

The PSi optical microcavity produced with the graded-index approach displays a narrow transmission line in the middle of the reflective stopband. An example of a typical reflectance spectrum is shown in **Figure 1**(a). The central wavelength (λ_c) of the

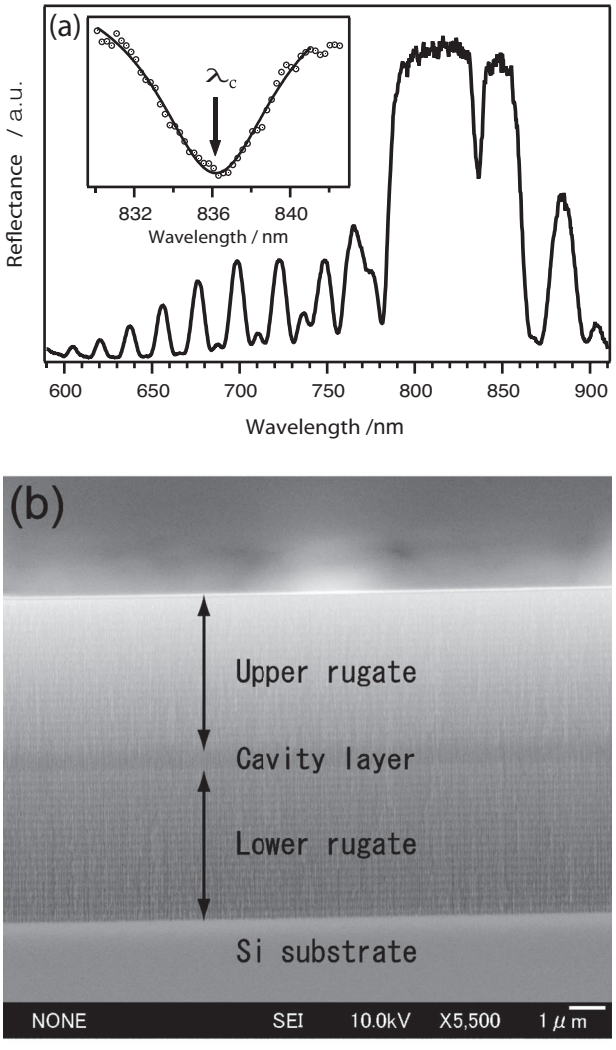

Figure 1. (a) Reflectance spectrum for a PSi optical microcavity. The microcavity layer produces a narrow transmission band that can be observed in the middle of the stopband. The inset shows a magnification of the cavity resonance with a Lorentzian fit to the experimental data. The position of the central wavelength λ_c can be determined with great reproducibility. (b) Cross-sectional SEM micrograph of a graded-index PSi microcavity, with the constant refractive index cavity layer in the middle.)

stopband dip is caused by resonance occurring in the cavity layer in the middle of the structure. The cavity layer can clearly be seen in Figure 1(b), which shows a cross-sectional SEM micrograph of a graded-index PSi sample. The resonant wavelength value (λ_c) can be easily determined by fitting a Lorentzian curve to the experimental data (Figure 1(a) inset). With the experimental set-up used in this work, Lorentzian fitting allowed us to determine the resonance position, with a smaller than 0.2 nm accuracy, between consecutive measurements. This is slightly smaller than the accuracy of the spectrophotometer given by the manufacturer.

The effect of TC and THC treatments on the reflectance spectra of microcavity samples is presented in **Figure 2**(a). Both surface modifications cause a small blue shift to the observed spectra, which can be attributed to slight decrease in the PSi effective refractive index value.[38] The overall shape of the spectra is preserved, indicating that the carbonization treatments do not cause a noticeable effect to the optical properties of the PSi samples. For the TC treated samples, a small decrease in the intensity of sidelobes outside the reflective stopband is observed for shorter wavelengths. This might be caused by a slight increase in the optical absorption coefficient of the material.

Figure 2(b) demonstrates the effect of modification with undecylenic acid (UnPSi) and the two-step UnTHC treatment on as-anodized PSi sample reflectance spectra. In both cases a redshift of the cavity resonance is observed, which is attributed to the formation of a monolayer of undecylenic acid on the inner surface of the porous samples. UnPSi treatment on as-anodized samples results in a larger redshift in comparison to the total shift observed for the UnTHC treated samples. However, as the initial THC treatment causes a blueshift, the redshift attributed to undecylenic acid binding on as-anodized or THC treated PSi surface is roughly the same. Effects of surface treatments on the resonant wavelength (λ_c) of PSi microcavities are summarized in **Table 1**. As can be seen from Table 1, the resonant wavelength shift ($\Delta\lambda_c$) due to surface modification is more reproducible for TC and THC treatments. This is probably due to slight differences in the amount of covalently attached undecylenic acid between the -COOH -derivatized samples. However, all the modified PSi microcavity samples retain sufficient optical properties, which should allow for accurate chemical sensing.

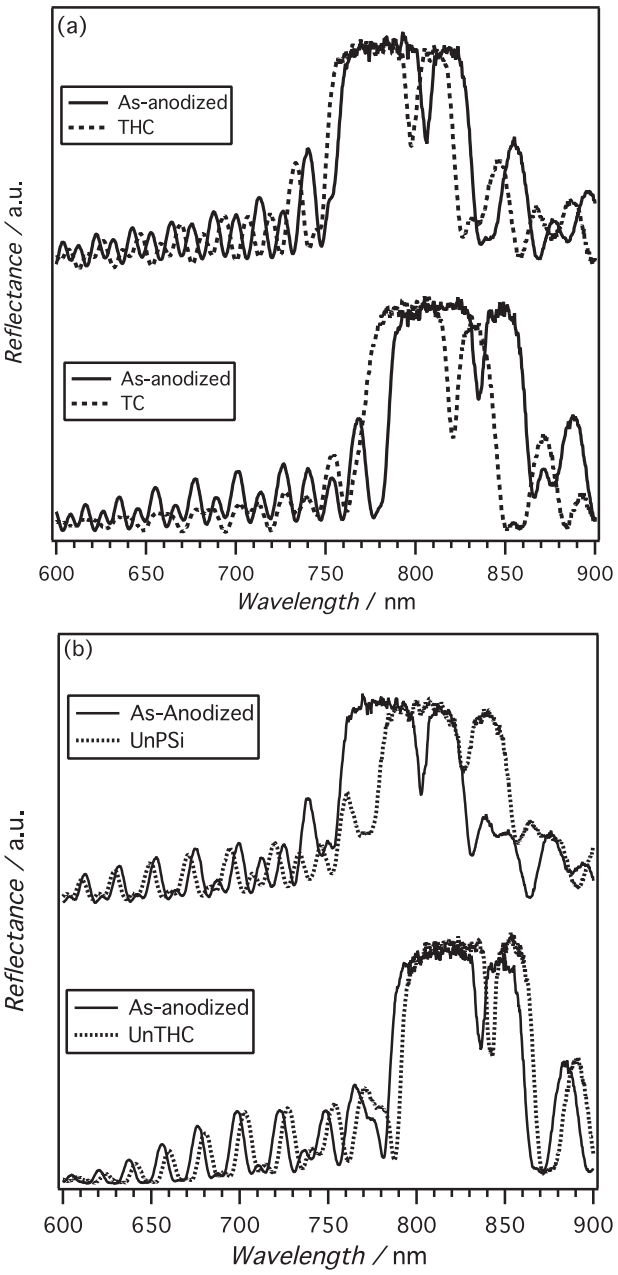

Figure 2. (a) Effect of THC and TC treatments on the reflectance spectra of PSi optical microcavities. (b) Effect of UnPSi and UnTHC treatments on reflectance spectra. The carbonization treatments cause a slight blueshift, whereas undecylenic acid functionalization results in a redshift of the spectra in both cases.)

2.2. Stability and Vapor Sensing

Stability and sensitivity towards ethanol and amine vapors was examined by subjecting the samples consecutively to a lower and higher concentration of EtOH, MA, and TMA vapors (in that order) for 5 min, respectively. The samples were allowed to recover after each sensing cycle for a minimum of 20 min (at least 1.5 h in the case of amines). Reflectance spectra were recorded before, during, and after vapor exposure. Changes in the resonant cavity wavelength (λ_c) position were monitored as a function of time. Volumetric vapor concentrations are shown in **Table 2**.

A typical experiment, where UnTHC samples are exposed to methylamine vapor, is shown as an example in **Figure 3**(a). After obtaining a reference zero-point for the redshifts with two consecutive measurements, the samples were exposed to methylamine for a period of 5 min. Sample recovery was then monitored by measuring spectra under nitrogen flow for a period of 35 min. From Figure 3(a) one can see that the response of the UnTHC treated sample to MA vapor has reached a steady state within one minute. The obtained redshifts also grow as a function of vapor concentration and remain stable through the 5 min exposure time. The redshifts in Figure 3(a) are depicted as average values for two samples. Judging by the relatively small error bars (standard deviation), it is obvious that the obtained response is quite reproducible. Sample recovery is considerably

Table 1. (Change in the resonant wavelength value (λ_c) of the microcavity after different surface treatments. Arithmetic mean values for two samples are shown along with standard deviation. Even though the number of samples is far too small for conducting proper statistical analysis, the values presented here still offer a convenient way for roughly assessing the reproducibility of the treatments)

Sample	$\Delta\lambda_c$ [nm]
THC	−8.06 ± 0.12
TC	−14.5 ± 0.2
UnTHC	9.7 ± 5.1
UnPSi	22.7 ± 2.4

slower in comparison to response time, which can be explained with hysteresis caused by capillary condensation of the studied vapor inside the pores and, especially in the case of amine molecules, a tendency to stick on sample surface.[37,42]

An identical experiment for UnPSi samples is shown in Figure 3(b) for comparison. In this case, instead of average values the measured redshift values for the two UnPSi samples are shown independently. For sample 1 (Figure 3(b)) a similar behavior to UnTHC samples is observed, where a redshift is first observed as the sample is subjected to MA vapor. However, during the exposure the λ_c values start to slowly blueshift. As the MA flow is cut off, the resonant wavelength value quickly returns to the original value. This is followed by a progressive blueshift as the sample is allowed to recover under nitrogen flow. For sample 2 (Figure 3(b)), an immediate blueshift is observed when the sample is exposed to lower MA concentration. After MA exposure a progressive blueshift of λ_c is observed, which reaches a value of 20 nm 35 min after MA exposure. This blueshift for both UnPSi samples can be attributed to either oxidation or partial dissolution of the samples.[30] When sample 2 is exposed to a higher concentration of MA a similar redshift is observed as for sample 1 (Figure 3(b)). This is again followed by a large blueshift. It should be noted that the zero-point is corrected for blueshift between the two measurements to correspond with the new blueshifted λ_c value. The observed differences in oxidation behavior between samples 1 & 2 can be explained by differences in measurement procedure. Sample 1 was allowed to recover overnight from the initial sensing experiments with EtOH vapor (conducted prior to MA exposure), whereas for sample 2 the MA sensing experiments were conducted immediately after the sample had recovered from EtOH exposure. Indeed, when the zero-point-drift for sample 1 is inspected, an overnight blueshift in the order

Table 2. (Volumetric vapor concentrations for the different chemicals used in sensing experiments, verified with FTIR measurements (EtOH) and gas-liquid chromatography (MA and TMA)).

Vapor	Low Concentration	High Concentration
EtOH	0.57 ± 0.01%	1.03 ± 0.04%
MA	4.98 ± 0.25%	10.7 ± 0.16%
TMA	7.19 ± 0.29	13.9 ± 0.42%

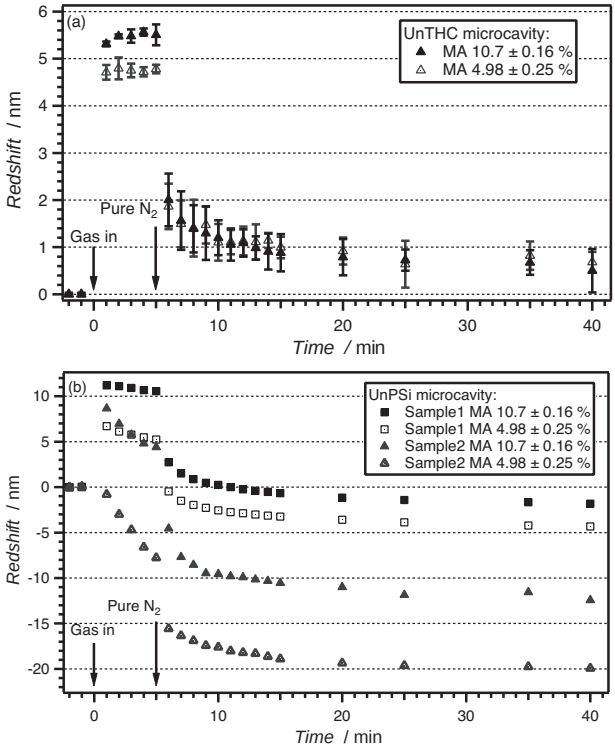

Figure 3. Recorded resonant wavelength redshifts as a function of time for UnTHC (a) and UnPSi (b) microcavity samples, when the samples were exposed to two different concentrations of methylamine vapor. UnTHC samples display a reproducible response with relatively fast recovery, whereas a considerable zero-point-drift is observed for the UnPSi samples.)

of 50 nm is observed. As for sample 2, progressive oxidation occurs during the MA sensing measurements, and at the beginning of TMA measurements an equally large λ_c blueshift as for sample 1 is recorded. In order to clarify the effect of the measurement procedure, we performed a control experiment, where a freshly prepared UnPSi rugate filter was exposed directly to MA vapor, without prior EtOH exposure, showed similar behavior as sample 1 (Figure 3(b)). More detailed qualitative analysis on sample oxidation is discussed in section 2.3.

All sensing results for four different sample types are included as supplementary material. In contrast to UnPSi samples, TC, THC, and UnTHC samples do not display zero-point blueshift during and after exposure to EtOH, MA, and TMA vapors. This indicates that these samples are considerably more stable in comparison to UnPSi microcavities. The average redshifts measured for TC, THC, and UnTHC microcavities in response to EtOH, MA, and TMA vapors are shown in **Figure 4**. TCPSi samples displayed largest sensitivity towards all studied vapors. In the case of amines, THC showed the smallest response, whereas UnTHC sample sensitivity was in between the two. We expected that amines might form a hydrogen bond with the carboxyl group, which would increase UnTHC sample sensitivity towards amines. However, considering the relatively fast recovery of UnTHC samples from amine exposure, this does not seem to be the case. Instead, sample sensitivity is more likely strongly connected to the hydrophilic character of

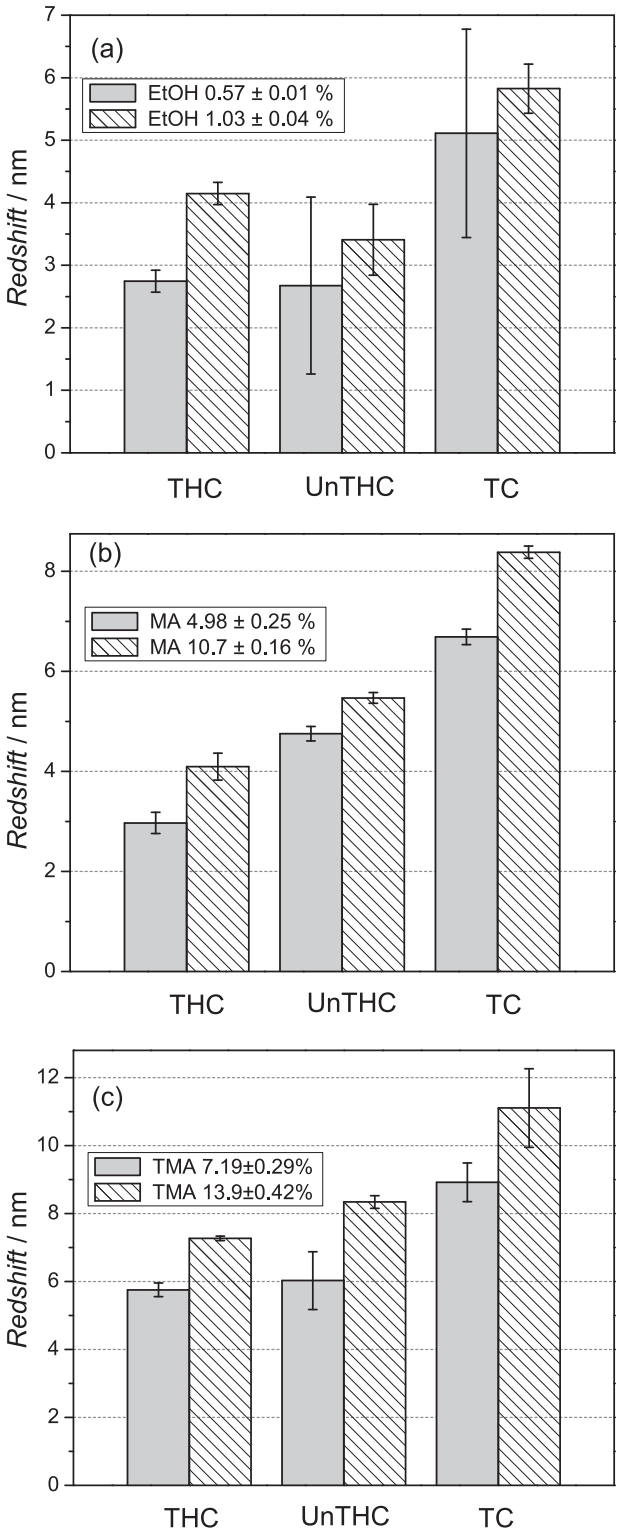

Figure 4. Recorded average redshifts for samples with THC, UnTHC, and TC modified surface, when exposed to two different concentrations of ethanol (a), methylamine (b), and trimethylamine (c) vapor. Error bars indicate the calculated standard deviation values.)

the modified PSi surfaces. THC treatment is known to result in hydrophobic surfaces whereas TC treatment produces a hydrophilic surface.[33,42] Functionalization of THC surface with undecylenic acid on the other hand tunes the hydrophilic character of the samples in between TC and THC treated surfaces. As both solutions of MA and TMA are mixed into water, vaporization used in the sensing experiments results in a mixture of humidity and amine vapors.

When sensitivity towards ethanol is examined (Figure 4(a)), THC samples display a larger redshift than UnTHC samples. For TCPSi samples a large variation between the two samples is observed when they are exposed to EtOH. Anomalously the second TC treated sample seems to produce a larger redshift for the smaller EtOH concentration. However, the difference between the two samples is clearly reduced after the first sensing cycle, and the response to higher ethanol concentration seems to be roughly equal for both samples. The λ_c values do not seem to fully recover to their initial positions after the first exposure, but remain slightly redshifted. This observation is probably caused by surface oxidation of the TCPSi samples. This might also be the cause for the ageing phenomenon that has been observed for TCPSi humidity sensors.[35] Indeed, measurements done with aged TCPSi microcavities indicate improved reproducibility between the samples with slightly increased redshift values adjusted to 5.87 ± 0.37 nm and 7.19 ± 0.93 nm for the lower and higher ethanol vapor concentrations, respectively. The topic of TCPSi surface oxidation is discussed more in sections 2.3. and 3. A rather large difference between the two UnTHC samples is also observed in the case of EtOH. This might also be related to some small changes in surface composition. In general, TC, THC, and UnTHC treated PSi microcavities provided fairly reproducible results, both in terms of reproducibility for a single sample, and reproducibility between two samples with similar surface modification. Out of all the surface modifications, THC treated samples displayed the highest reproducibility.

2.3. X-ray Photoelectron Spectroscopy

Excellent chemical stability is required from PSi sensors that are to be used under basic conditions. For example many amines, like MA and TMA used in this study, produce highly alkaline environments as they condensate inside the pores. Under these conditions the Si surface is highly susceptible to oxidation, and to make matters worse, silicon oxide dissolves in basic solutions.[20] In order to qualitatively assess sample stability, XPS measurements were used to study possible chemical changes in the surface modified PSi samples caused by the sensing experiments. The XPS survey spectra measured for freshly prepared chemically modified samples showed clear peaks for carbon and oxygen, in addition to silicon. In comparison, an as-anodized PSi sample with no surface modifications only showed traces of oxygen and carbon, and clear Si related peaks. Trace amounts of fluorine were also detected for all sample types. This is most likely due to residual fluorine from the PSi preparation process. C1s core level spectra for the surface treated samples show a dominant peak at around 285 eV, for all four sample types. Slight differences in the shape of the peak reflect the differences in the chemical binding states of different type of samples. Moreover, the spectra for UnTHC and UnPSi samples also reveal a smaller peak corresponding to an approximate binding energy of 289.5 eV (**Figure 5**). This

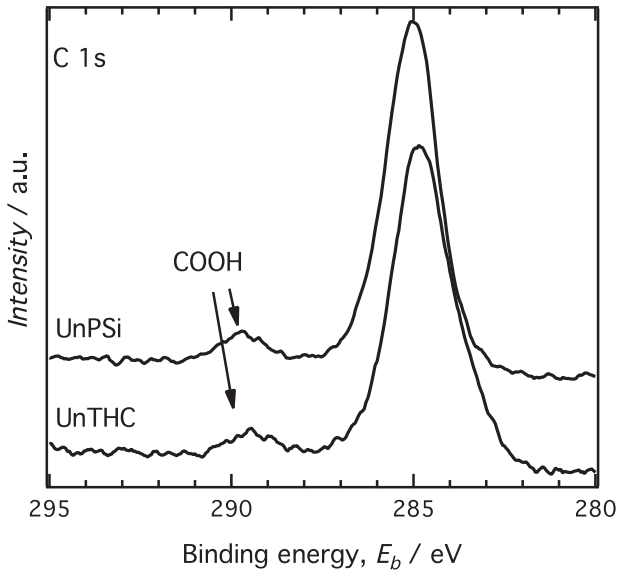

Figure 5. High resolution C 1s region XPS spectra for freshly prepared UnPSi and UnTHC microcavity samples (the spectra are vertically shifted for clarity). The smaller peak situated close to 289.5 eV is assigned to carboxyl group and is clearly visible for both sample types.)

small peak is assigned to the carboxyl functional group.[29] After the sensing experiments a small decrease in the intensity of the carboxyl group related peaks is observed for both UnPSi and UnTHC samples (data not shown).

A significantly larger difference can be observed in the high-resolution Si 2p XPS spectra. Peak fitting and experimental data for UnPSi and UnTHC samples before and after sensing experiments is shown in **Figure 6**. For freshly prepared UnPSi and UnTHC samples the dominant peak at 99.48 eV (Figure 6(a)) and 99.20 eV (Figure 6(c)) is unambiguously assigned to silicon, whereas the smaller peak situated between 101.91–103.18 eV is caused by SiO_2.[43,44] Boukherroub et al. did not observe the oxide related peak for UnPSi,[29] so it is quite likely that the small peak in UnPSi is due to slight atmospheric oxidation that has occurred after sample preparation. Photoelectron spectrum measured after the sensing experiments reveals a large increase in the SiO_2 related peak for the UnPSi sample (Figure 6(b)). This confirms that the large blueshift of the microcavity resonant wavelength, which was observed during the sensing experiments (Figure 3(b)), is mostly caused by considerable oxidation. The UnTHC sample spectrum (Figure 6(d)) shows a much smaller change with only a slight increase in the oxide related peak intensity. These results clearly indicate the superior stability of the UnTHC treated sample over the UnPSi sample. The small peaks in the middle (Figure 6(a, c, and d)) are more difficult to resolve, but they could be assigned to Si-C, O-Si-C, or alternatively to some combination of the two.[44] This is demonstrated in Figure 6(c) and (d).

When examining the Si2p core level spectra for TC- and THC-PSi samples after sensing experiments (Figure S5), we observe that the oxide related peak in the THC sample has not grown considerably whereas for the TC sample a clear increase is observed. For comparison, Si2p photoelectron spectra for freshly prepared TC- and THC-PSi can be found from reference.[45] As noted in section 2.2, no zero-point blueshift was observed in the sensing experiments for the TC treated sample. Instead a slight zero-point redshift was observed. This would suggest a formation of an oxide layer on the outer surface of the pore walls. This conclusion is supported by the observation of a contribution that can be assigned to a C-O-C bridge in the O1s core level spectrum for the TC sample. Moreover, despite the TCPSi oxidation no charge compensation was needed during the XPS measurements, which indicates that the higher conductivity in comparison to the THC surface was preserved after sensing experiments.[46]

As expected, XPS spectra for THC and UnTHC treated samples bear a great resemblance, with the notable exception of the carboxyl group related feature in C1s core level spectrum of UnTHCPSi (Figure 5). Differences can also be found from the O1s photoelectron spectra, where a contribution assignable to C = O[44] (carbonyl group) can be distinguished for the UnTHC sample.

3. Discussion

Variation in the recovery time during the sensing experiments was quite large between the two TC samples. This might be related to hydrophilic character of the TC surface. Our previous studies with an electrical TCPSi gas sensor have also shown that MA and TMA have a high affinity towards the carbonized surface.[37] Also the formation of the thin oxide layer on the carbonized surface during the sensing experiments plays a role. A post-TC oxidation treatment before the sensing experiments should improve the reproducibility for the TCPSi sensors. Surface oxidation also seems to improve sensitivity, which might be connected with increased hydrophilicity and slight reduction in average pore diameter, which, in turn, promotes capillary condensation of vapors inside the pores. The average pore size was confirmed to be roughly around 10 nm with SEM measurements. Nitrogen sorption measurements give similar values for the average pore size.[36,41] Pore size distributions in this size range always include a small fraction of pores with a diameter in the order of a few nanometers, where capillary condensation effects are expected to occur.[36]

The response and recovery of the THC and UnTHC samples was fairly reproducible, with some exceptions in EtOH sensing. The UnPSi samples displayed a large blueshift during the experiments. This can be attributed to oxidation. When the UnPSi samples were subjected to TMA vapor (Figure S4), the oxidation rate had already slowed down and no zero-point blueshift was observed. For both the UnPSi and UnTHC samples, a slight decrease in the COOH related peak in C1s XPS spectra is observed. A plausible explanation might be that small amounts of undecylenic acid are removed from the surface during the experiments due to highly alkaline experimental conditions.

The biggest difference between the UnPSi and UnTHC samples is their stability against oxidation. Also as the carboxylic acid related features in UnTHC XPS-spectra are slightly less prominent, the amount of undecylenic acid bound on the surface is evidently slightly smaller. However, as the sample stability is greatly increased, the UnTHC treatment is a promising method for producing stable biosensors from PSi.

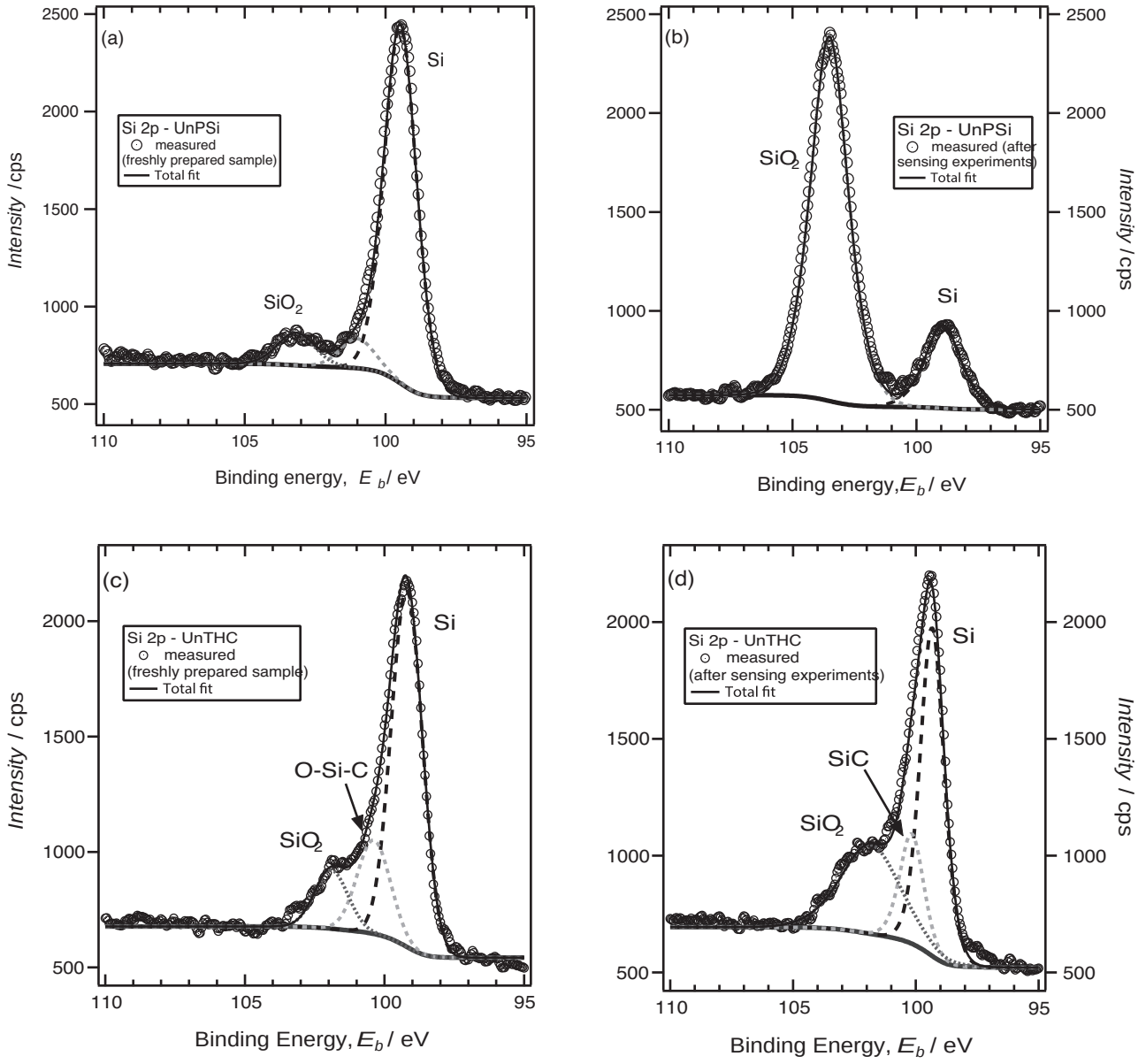

Figure 6. XPS-spectra for UnPSi and UnTHC samples, measured before (a and c), and after (b and d) the vapor sensing experiments. UnPSi microcavity samples (a and b) undergo substantial oxidation during the sensing experiments. Only a slight increase in SiO_2 related peak is observed in the case of UnTHC treated samples (c and d).)

4. Conclusions

Simple and reproducible production of graded-index microcavities from PSi was demonstrated. Chemical modification of the samples was found feasible with all four treatment-methods studied. The surface treatments result in differences when the samples were used in vapor sensing of EtOH, MA, and TMA. TC, THC, and UnTHC treated samples showed considerably higher stability in comparison to the UnPSi samples under the harsh experimental conditions. Sensitivity was also greatly affected by the chemical modifications. The differences in the hygroscopic character of the samples are most likely largely responsible for the observed differences. An oxide layer formation during the experiments was observed for the TC samples. This caused some variation in the sensing experiments. UnTHC and THC treated samples showed good reproducibility and only slight oxidation during the experiments. Based on the results the UnTHC treatment seems extremely promising for fabricating PSi based biosensors with greatly improved stability.

5. Experimental Section

Materials: Boron-doped monocrystalline p^+-type silicon wafers ((100) polished) with 0.005-0.03 Ωcm resistivity were purchased from

Ferrotec Corp. Aqueous HF ((46-48 wt%)) was purchased from Stella Chemifa Corp. Dichloromethane, ethanol, methylamine (40% in water), tetrahydrofuran, and trimethylamine (30% in water) were acquired from Nacalai Tesque, Inc. Undecylenic acid was purchased from Sigma-Aldrich. HCl and NaOH aqueous solutions were purchased from Wako Pure Chemical Industries, Ltd.

Sample Preparation: Samples were prepared by electrochemical anodization of p^+-type silicon substrates. InGa alloy was applied on backside of the Si substrate in order to ensure an ohmic contact with the current collector. The substrate was placed in a teflon cell with a 0.79 cm^2 area of the substrate surface exposed to the electrolyte. A copper plate was placed under the Si substrate, and used as a current collector for the working electrode. Electrolyte solution composed of hydrofluoric acid (46-48 wt%) and ethanol in 1:1.7 volumetric-ratio was used. The working electrode and a platinum counter electrode were connected to a programmable current source (Keithley 6221), which was used for controlling the anodization process. Sinusoidal anodization current, with current density values oscillating between 63.3 and 113.9 mA cm^{-2}, was applied for 19.75 -times with 5 s period length. A cavity layer was formed subsequently by applying a fixed 63.3 mA cm^{-2} anodization current density for 12.5 s. Finally, a second sinusoidal current form (identical to the first one, but with a 270° phase shift) was applied to produce the second reflector below the cavity layer. After the anodization process, the samples were rinsed with ultrapure water (Millipore, Milli-Q Gradient) and ethanol, and carefully dried with nitrogen gas.

Surface Modifications: Thermal hydrocarbonization (THC) was performed, by placing the dried samples in a quartz tube. The samples were kept under constant nitrogen flow (1 L min^{-1}) for over 30 min. An acetylene flow (1 L min^{-1}) was introduced to the tube 10 min prior to heat treatment. The quartz tube was inserted into a tube furnace set at 500 °C for 15 min. The acetylene flow was cut off 30 s before evacuating the quartz tube from the furnace. The samples were allowed to cool down to room temperature under nitrogen flow.

Thermal carbonization (TC) was performed using a two-step treatment process [36] where the first step was the hydrocarbonization treatment, which was conducted as described above. After the hydrocarbonized samples had cooled down inside the quartz tube under nitrogen flow, acetylene flow was introduced again in tandem with the nitrogen flow for 15 min. The acetylene was cut off and after a 30 s waiting period the quartz tube was inserted inside the tube furnace set at 820 °C. The heat treatment was applied for 10 min, after which the quartz tube was removed from the furnace and the samples were allowed to cool down to room temperature under constant nitrogen flow.

Two differing carboxylic acid addition treatments were performed, by modifying as-anodized and THC treated samples, respectively. The THCPSi samples were immersed in neat undecylenic acid solution for 12 hours at 110 °C. Afterwards, the thermally hydrocarbonized samples, functionalized with undecylenic acid (UnTHC), were rinsed copiously with ethanol and dichloromethane in order to remove excess undecylenic acid. In the case of as-anodized samples, modification with undecylenic acid was conducted by inserting the dried samples in a round-bottom flask together with neat undecylenic acid solution. The flask was connected to a Schlenk line and purged with three vacuum-refill cycles. The samples were then allowed to react under argon atmosphere for 20 h at 110 °C. The resulting undecylenic acid functionalized PSi (UnPSi) samples were copiously rinsed with dicholoromethane and tetrahydrofuran, and dried under a stream of nitrogen.

Sample Characterization and Sensing Set-Up: Reflectance measurements were conducted with an Ocean Optics HR4000CG-UV-NIR spectrometer, coupled to a tungsten halogen light source (LS-1, Ocean Optics). A bifurcated optical fiber was used for illuminating the sample, at normal angle of incidence, and collecting the reflected light to the spectrometer. Scanning electron microscopy (JEOL JSM-6500FE) was employed for examination of the optical microcavities. Sample surface was analyzed with X-ray photoelectron spectroscopy (JEOL JPS-9010MC). Al Kα line (1486.6 eV) was used as X-ray source, which was operated at 10 kV and 10 mA (100 W). During the XPS measurements, samples were kept in high vacuum up to 10^{-7} Pa. Obtained binding energies were referenced to adventitious carbon C1s signal at 284.5 eV.

The sensing experiments were conducted by mounting the samples in an atmospheric chamber equipped with an optical window. Vapor concentration inside the chamber was controlled, by adjusting relative gas-flow ratios with mass-flow controllers. Nitrogen was used as carrier gas [47]. The ethanol vapor concentrations were determined with FTIR spectrometer (Jasco, FT/IR-460 Plus) by using the Beer-Lambert law. The amine concentrations were determined with gas-liquid chromatography (GLC) measurements. GLC analysis was performed on a Shimadzu GC-14B instrument equipped with a flame ionization detector and a CP-Volamine capillary column (Agilent, 30 m × 0.32 mm). The determination of concentration was performed by directing the gas stream (nitrogen and amine) inside 20 mL of 1.0 M HCl aqueous solution for 1 min. 0.1% of phenolphthalein solution (approximately 90% ethanol, 200 μL), and isopropanol (42.0 μL, 0.500 mmol) which acted as an internal reference, were added to the solution. Back titration was performed with NaOH (1.0 M) aqueous solution and was used for confirming the results. NaOH solution was added slightly in excess (ca 21 mL) and the solution was analyzed with GLC.

Supporting Information

Supporting Information is available from the Wiley Online Library or from the author.

Acknowledgements

This work was partially supported by the Grant-in-Aid from the Japan Society of Promotion of Science for Scientific Research (B) under Grant No. 22350092. The authors would like to thank assistant Prof. Masayuki Wakioka and Prof. Fumiyuki Ozawa from Kyoto University for assistance with GLC measurements. T. Jalkanen acknowledges financial support from MEXT, the Japanese Ministry of Education, Culture, Sports, Science & Technology. Supporting Information is available online from Wiley InterScience or from the author.

Received: February 8, 2012
Revised: April 5, 2012
Published online: May 25, 2012

[1] P. A. Snow, E. K. Squire, P. St. J. Russell, L. T. Canham, *J. Appl. Phys.* **1999**, *86*, 1781.
[2] M. S. Salem, M. J. Sailor, K. Fukami, T. Sakka, Y. H. Ogata, *J. Appl. Phys.* **2008**, *103*, 083516.
[3] V. S.-Y. Lin, K. Motesharei, K.-P. S. Dancil, M. J. Sailor, M. R. Ghadiri, *Science* **1997**, *278*, 840.
[4] C. Pacholski, M. Sarton, M. J. Sailor, F. Cunin, G. M. Miskelly, *J. Am. Chem. Soc.* **2005**, *127*, 11636.
[5] V. Torres-Costa, R. J. Martín-Palma, *J. Mater. Sci.* **2010**, *45*, 2823.
[6] S. Chan, P. M. Fauchet, Y. Li, L. J. Rothberg, B. L. Miller, *Phys. Status Solidi A* **2000**, 1*82*, 541.
[7] C. Baratto, G. Faglia, G. Sberveglieri, Z. Gaburro, L. Pancheri, C. Oton, L. Pavesi, *Sensors* **2002**, *2*, 121.
[8] E. Estephan, M.-B. Saab, V. Agarwal, F. J. G. Cuisinier, C. Larrogue, C. Gergelly, *Adv. Funct. Mater.* **2011**, *21*, 2003.
[9] S. Frohnhoff, M. G. Berger, *Adv. Mater.* **1994**, *6*, 963.
[10] V. Pellegrini, A. Tredicucci, C. Mazzoleni, L. Pavesi, *Phys. Rev. B* **1995**, *52*, 14328.
[11] L. Pavesi, G. Panzarini, L. C. Andreani, *Phys. Rev. B* **1998**, *58*, 15794.
[12] P. J. Reece, G. Lérondel, W. H. Zheng, M. Gal, *Appl. Phys. Lett.* **2002**, *81*, 4895.
[13] M. Ghulinyan, C. J. Oton, G. Bonetti, Z. Gaburro, L. Pavesi, *J. Appl. Phys.* **2003**, *93*, 9724.
[14] K. J. Vahala, *Nature* **2003**, *424*, 839.
[15] S. Weiss, P. M. Fauchet, *IEEE J. Sel. Top. Quant.* **2006**, *12*, 1514.

[16] B. G. Bovard, *Appl. Optics* **1993**, *32*, 5427.
[17] M. G. Berger, R. Arens-Fischer, M. Thönissen, M. Krüger, S. Billat, H. Lüth, S. Hillbrich, W. Theiß, P. Grosse, *Thin Solid Films* **1997**, *297*, 237.
[18] E. Lorenzo, C. J. Oton, N. E. Capuj, M. Ghulinyan, D. Navarro-Urrios, Z. Gaburro, L. Pavesi, *Appl. Optics* **2005**, *44*, 5415.
[19] M. M. Hawkeye, M. J. Brett, *J. Appl. Phys.* **2006**, *100*, 044322.
[20] M. J. Sailor, in *Porous Silicon in Practice*, Wiley-VCH, Weinheim, **2011**.
[21] J. M. Buriak, *Adv. Mater.* **1999**, *11*, 265.
[22] M. P. Stewart, J. M. Buriak, *Adv. Mater.* **2000**, *12*, 859.
[23] J. Salonen, V.-P. Lehto, *Chem. Eng. J.* **2008**, *137*, 162.
[24] A. M. Ruminski, B. H. King, J. Salonen, J. L. Snyder, M. J. Sailor, *Adv. Funct. Mater.* **2010**, *20*, 2874.
[25] J. M. Buriak, M. J. Allen, *J. Am. Chem. Soc.* **1998**, *120*, 1339.
[26] M. P. Stevart, J. M. Buriak, *Angew. Chem. Int. Ed.* **1998**, *37*, 3257.
[27] J. E. Bateman, R. D. Eagling, D. R. Worrall, B. R. Horrocks, A. Houlton, *Angew. Chem. Int. Ed.* **1998**, *37*, 2683.
[28] R. Boukherroub, S. Morin, D. D. M. Wayner, F. Bensebaa, G. I. Sproule, J.-M. Baribeau, D. J. Lockwood, *Chem. Mater.* **2001**, *13*, 2002.
[29] R. Boukherroub, J. T. C. Wojtyk, D. D. M. Wayner, D. J. Lockwood, *J. Electrochem. Soc.* **2002**, *149*, 59.
[30] I. N. Lees, H. Lin, C. A. Canaria, C. Gurtner, M. J. Sailor, G. M. Miskelly, *Langmuir* **2003**, *19*, 9812.
[31] J. Salonen, V.-P. Lehto, M. Björkqvist, E. Laine, L. Niinistö, *Phys. Status Solidi A* **2000**, *182*, 123.
[32] J. Salonen, E. Laine, L. Niinistö, *J. Appl. Phys.* **2002**, *91*, 456.
[33] J. Salonen, M. Björkqvist, E. Laine, L. Niinistö, *Appl. Surf. Sci.* **2004**, *225*, 389.
[34] M. Björkqvist, J. Salonen, J. Paski, E. Laine, *Sensor. Actuat. A-Phys.* **2004**, *112*, 244.
[35] J. Salonen, J. Tuura, M. Björkqvist, V.-P. Lehto, *Sensor. Actuat. B-Chem.* **2006**, *114*, 423.
[36] J. Tuura, M. Björkqvist, J. Salonen, V.-P. Lehto, *Sensor. Actuat. B-Chem.* **2008**, *131*, 627.
[37] M. Björkqvist, J. Salonen, J. Tuura, T. Jalkanen, V.-P. Lehto, *Phys. Status Solidi C* **2009**, *6*, 1769.
[38] V. Torres-Costa, R. J. Martín-Palma, J. M. Martínez-Duart, J. Salonen, V.-P. Lehto, *J. Appl. Phys.* **2008**, *103*, 083124.
[39] T. Jalkanen, V. Torres-Costa, J. Salonen, M. Björkqvist, E. Mäkilä, J. M. Martínez-Duart, V.-P. Lehto, *Opt. Express* **2009**, *17*, 5446.
[40] B. Sciacca, S. D. Alvarez, F. Geobaldo, M. J. Sailor, *Dalton T.* **2010**, *39*, 10847.
[41] M. Kovalainen, J. Mönkäre, E. Mäkilä, J. Salonen, V.-P. Lehto, K.-H. Herzig, K. Järvinen, *Pharm. Res.* doi:10.1007/s11095-011-0611- 6.
[42] M. Björkqvist, J. Paski, J. Salonen, V.-P. Lehto, *IEEE Sens. J* **2006**, *6*, 542.
[43] Y. Hijikata, H. Yaguchi, M. Yoshikawa, S. Yoshida, *Appl. Surf. Sci.* **2001**, *184*, 161.
[44] M. Omastová, K. Boukerma, M. Chehimi, M. Trchová, *Mater. Res. Bull.* **2005**, *40*, 749.
[45] M. Sarparanta, E. Mäkilä, T. Heikkilä, J. Salonen, E. Kukk, V.-P. Lehto, H. A. Santos, J. Hirvonen, A. J. Airaksinen, *Mol. Pharm.* **2011**, *8*, 1799.
[46] J. Salonen, M. Björkqvist, J. Paski, *Sensor. Actuat. A-Phys.* **2004**, *116*, 438.
[47] T. Jalkanen, J. Salonen, V. Torres-Costa, K. Fukami, T. Sakka, Y. H. Ogata, *Opt. Express* **2011**, *19*, 13291.